Acoustic-Domain Self-Interference Cancellation for Full-Duplex Underwater Acoustic Communication Systems

Yanyan Wang*, Yingsong Li*, Lu Shen† and Yuriy Zakharov†
* College of Information and Communication Engineering, Harbin Engineering University, Harbin 150001, China
E-mail: wangyanyan@hrbeu.edu.cn, liyingsong@ieee.org
† Department of Electronic Engineering, University of York, York YO10 5DD, United Kingdom
E-mail: ls1215@york.ac.uk, yury.zakharov@york.ac.uk

Abstract—**In full-duplex (FD) underwater acoustic communication (FD-UWAC) systems, the self-interference (SI) will affect the communication performance. Till now, there is no solution for active cancellation of the wide-band SI in the acoustic domain. In this paper, we propose such a solution with two transducers, a primary transducer and a secondary transducer. The acoustic signal emitted by the secondary transducer is generated to cancel the SI signal received at the hydrophone from the primary transducer. The performance of the proposed scheme is investigated by simulation. We use the Waymark UWA simulator that allows the virtual signal transmission in various acoustic environments. The simulation results demonstrate that the proposed scheme can provide an effective acoustic SI cancellation for FD-UWAC systems, in terms of the mean square error and bit error ratio.**

I. Introduction

Underwater acoustic communication (UWAC) attracts extensive attention due to its wide applications for monitoring marine environments and marine exploration. However, the throughput of UWAC is limited by the extremely narrow available bandwidth [1, 2]. In order to improve the spectral efficiency in terrestrial radio communication systems, the full-duplex (FD) technology has been introduced [3, 4]. The FD operation improves the throughput by transmitting and receiving signals simultaneously in the same frequency bandwidth. However, the self-interference (SI) is the biggest challenge in FD systems, when the near-end transmission interferes with a weak far-end signal of interest. In order to accurately receive the far-end signal, the SI should be cancelled to a level comparable to the level of the ambient noise.

The SI cancellation can be done in the analogue and/or digital domains. In some applications to FD terrestrial radio communications, a combination of analogue and digital cancellation is used, which achieves a superior cancellation performance [3–6]. The analogue cancellation is implemented before analog-to-digital conversion (ADC) to avoid the signal saturation due to the limited ADC resolution [4, 5, 7]. After that, the digital cancellation is carried out to cancel the residual SI after the analogue cancellation [3, 8, 9]. The amount of the digital cancellation can achieve 20-45 dB [4, 5]. This amount of SI cancellation however would not be enough in many UWAC scenarios, where the difference in levels of the far-end and near-end signals can be as high as 100 dB.

In terrestrial radio communication systems, the SI cancellation in the radio domain is also used, which can be implemented using three antennas [4, 5, 10, 11]. The main idea is to separate two transmit antennas from the receiver antenna with distances of d and $d+\lambda/2$, where λ is a wavelength at the operating frequency, so that the signals from the two transmit antennas cancel each other at the receive antenna. However, in UWAC systems, due to wide bandwidth of communications signals and multipath propagation, such a scheme would have a low cancellation performance.

In FD-UWAC systems, a design is presented for SI cancellation, which combines the analogue and digital cancellation [12]. This design however does not provide a high cancellation performance. Additionally, some of FD acoustic designs are presented to increase communication throughput by frequency division or/and code division [13, 14]. However, these schemes do not increase the spectral efficiency.

In this paper, we propose a scheme for adaptive SI cancellation of wideband signals in the acoustic domain by using two transmit antennas and one receive antenna. The performance of the proposed scheme is investigated by numerical simulation. We use the Waymark simulator for UWA channels that provides the virtual signal transmission in user-defined acoustic environments [15]. The simulation results show that the proposed scheme can make the residual SI after acoustic cancellation close to the noise level. Therefore, the receiver can accurately demodulate the weak far-end communication signal of interest.

II. Acoustic-domain SI Cancellation

The FD-UWAC system with the proposed acoustic SI cancellation scheme is shown in Fig. 1. It operates at two different sampling rates. We use index i for samples with high sampling rate f_s and index n for samples with lower sampling rate f_d. We use the single-carrier communication signal with QPSK modulation. As an example, the carrier frequency is set to $f_c = 3072$ Hz, the symbol rate $f_d = 1024$ Hz, and the high sampling rate $f_s = 4f_c = 12288$ Hz. The transmitted QPSK

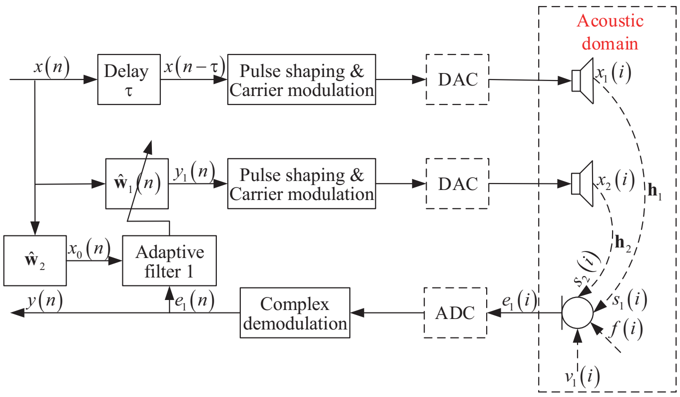

Fig. 1. The block diagram of acoustic SI cancellation for FD-UWAC system.

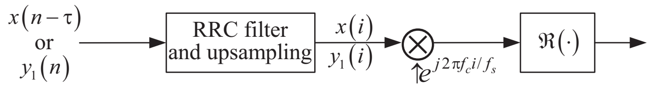

Fig. 2. Pulse shaping and carrier modulation; $\Re(\cdot)$ denotes the real part of a complex number.

symbols $x(n)$ are pulse-shaped by using the root-raised cosine (RRC) filter [16]; we set the roll-off factor to $\alpha = 0.2$ and the filter length of 14 symbols. The pulse-shaped baseband signal is up-sampled to the sampling rate f_s and modulates the carrier frequency f_c as illustrated in Fig. 2.

The FD-UWAC system contains two transducers. The first is used to transmit the data $x(n)$ intended for the far-end user. The acoustic signal $x_1(i)$ from this transducer causes the SI $s_1(i)$ at the receive hydrophone. The other transducer emits a signal $x_2(i)$ to produce the acoustic signal $s_2(i)$ at the receive hydrophone that cancels the SI from the first transducer. To this end, the original data $x(n)$ are pre-distorted in an adaptive filter with the weight vector $\hat{\mathbf{w}}_1(n)$. In this setup, we denote the primary and secondary acoustic channels as $\mathbf{h}_1$ and $\mathbf{h}_2$, respectively; both $\mathbf{h}_1$ and $\mathbf{h}_2$ are unknown.

The weight vector $\hat{\mathbf{w}}_1(n)$ is adapted in such a way that the transmitted data $x(n)$ after passing through the filter $\hat{\mathbf{w}}_1(n)$ and channel $\mathbf{h}_2$ form a signal $s_2(i)$ that cancels the acoustic SI $s_1(i)$ from the primary path. The delay τ in the chain to the first transducer compensates for a delay in the adaptive filter $\hat{\mathbf{w}}_1(n)$.

Note that, in our investigation, we ignore the quantization errors introduced by a digital-to-analog converter (DAC). This is acceptable for the low-frequency acoustic signals used for underwater communications, since, at these frequencies, high precision (up to 24 bits) DACs and ADCs are available in practice. Therefore in Fig. 1, we only show the places where the ADC and DACs should be incorporated.

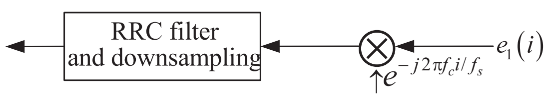

Fig. 3. Complex demodulation.

In the receiver, the hydrophone receives the signal

$$e_1(i) = s_1(i) + s_2(i) + f(i) + v_1(i), \qquad (1)$$

where $f(i)$ is a signal transmitted from the far-end, and $v_1(i)$ is the additive acoustic noise, which we assume white Gaussian. The passband received signal $e_1(i)$ after ADC and complex demodulation is transformed into the equivalent baseband signal $e_1(n)$ at the low sampling rate f_d. The complex demodulation is illustrated in Fig. 3.

The adaptive filter 1 in Fig. 1 uses the signal $e_1(n)$ as an error signal and tries to reduce its level as much as possible. In such a setup, the difference with classical adaptive filters (where all the processing is performed in the digital domain at the baseband) is that the error signal is generated in the acoustic domain at the passband, whereas the adaptation is performed in the digital domain at the baseband. The signal $x_0(n)$ plays the role of the regressor in the adaptive filter. Note that we could directly use the original data: $x_0(n) = x(n)$. However, our investigation has shown that this does not allow consistently high performance of the SI cancellation. Significantly better results are achieved if the regressor is generated by pre-filtering the data $x(n)$ in a filter $\hat{\mathbf{w}}_2$, which is a baseband estimate of the passband secondary path $\mathbf{h}_2$.

Therefore, the FD-UWAC system operates in two steps. In the first step, the secondary path is estimated, thus producing the weight vector $\hat{\mathbf{w}}_2$. In the second step, the adaptive filter produces the estimate $\hat{\mathbf{w}}_1(n)$, while the system simultaneously transmits near-end signal and receives the far-end signal with a 'frozen' weight vector $\hat{\mathbf{w}}_2$ obtained at the first step after convergence.

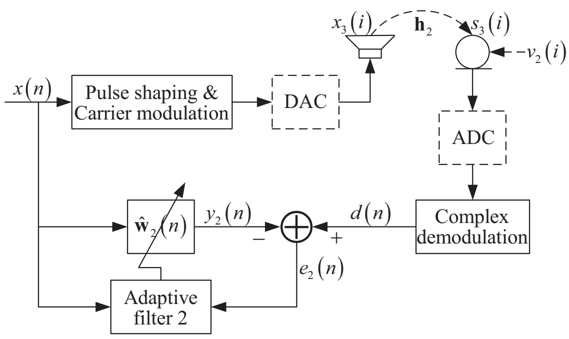

Fig. 4. Estimation of the secondary path $\mathbf{h}_2$.

For the first step, the adaptive filter 2 is used as shown in Fig. 4. A pseudo-noise QPSK sequence $x(n)$ is transmitted using the second transducer and received by the hydrophone. The received acoustic passband signal $s_3(i)$ is distorted by an additive noise $v_2(i)$. The demodulated baseband signal $d(n)$ is used as the desired signal, while the transmitted sequence of the QPSK symbols plays the role of the regressor. After the convergence of the adaptive filter, we obtain the weight vector $\hat{\mathbf{w}}_2$ as a baseband estimate of the secondary acoustic path $\mathbf{h}_2$.

The adaptive filter (adaptive filter 2 in Fig. 4) for the estimation of the vector $\mathbf{h}_2$ is the exponential window RLS algorithm implemented using the dichotomous coordinate descent (DCD) iterations [17]. The length L_2 of the adaptive filter is long enough to cover the length of the channel response $\mathbf{h}_2$ and the response of the RRC pulse-shape filter.

The performance of the processing is assessed using the normalized mean squared error (MSE), which is defined as

$$\mathrm{MSE}(n) = \frac{P_{e_2}(n)}{P_d}, \tag{2}$$

where $P_{e_2}(n) = |e_2(n)|^2$ is the instantaneous power of the error signal $e_2(n)$, and P_d is the average power of the received signal $d(n)$: $P_d = (1/M)\sum_{n=0}^{M-1} |d(n)|^2$, where $M \gg 1$. The signal-to-noise ratio (SNR) at the input to the receiver, in the first step, is defined as

$$\mathrm{SNR} = \kappa \frac{P_{s_3}}{\sigma_{v_2}^2}, \tag{3}$$

where P_{s_3} is the average power of the signal $s_3(i)$, $\sigma_{v_2}^2$ is the variance of the noise $v_2(i)$, and the factor $\kappa = f_s/(2f_d)$ takes into account the bandwidth of the transmitted signal.

The adaptation in the adaptive filter 1 in Fig. 1 is based on the error signal that is produced in the acoustic domain. Note that, in the classical form, the RLS algorithm computes the error signal as a difference between the desired signal and the adaptive filter output in the digital domain [18]. In our case, the error signal is generated in the acoustic domain at the hydrophone. Therefore, we use another form of the RLS algorithm as presented in Table I. This algorithm, if implemented directly as shown in Table I, would have a high complexity of $\mathcal{O}(L_1^3)$ arithmetic operations per iteration, where L_1 is the filter length. Instead of the direct approach, step 3 in Table I is implemented by solving the system of equations

$$\mathbf{R}(n)\Delta\hat{\mathbf{w}}(n) = \mathbf{x}_0(n)e_1^*(n) \tag{4}$$

with a few DCD iterations. With this approach, the complexity of the RLS adaptive filter is only $\mathcal{O}(L_1)$ arithmetic operations per iteration [17].

TABLE I
THE MODIFIED RLS ALGORITHM FOR ACOUSTIC SI CANCELLATION

Step	Equation
	Initialization: $\hat{\mathbf{w}}_1(-1) = \mathbf{0}$, $\mathbf{R}(-1) = \mathbf{\Pi}$, $\mathbf{x}_0(0) = \mathbf{0}$
	for $n = 0, 1, 2, \cdots$
1	$\mathbf{x}_0(n) = \mathbf{x}^H(n)\hat{\mathbf{w}}_2(n)$
2	$\mathbf{R}(n) = \lambda_1\mathbf{R}(n-1) + \mathbf{x}_0(n)\mathbf{x}_0^H(n)$
3	$\Delta\hat{\mathbf{w}}(n) = \mathbf{R}^{-1}(n)\mathbf{x}_0(n)e_1^*(n)$
4	$\hat{\mathbf{w}}_1(n) = \hat{\mathbf{w}}_1(n-1) + \Delta\hat{\mathbf{w}}(n)$

We evaluate the FD performance of the proposed SI canceller at step 2 using the normalized MSE defined as:

$$\mathrm{MSE}(n) = \frac{P_{e_1}(n)}{P_{s_1}}, \tag{5}$$

where $P_{e_1}(n) = |e_1(n)|^2$ is the instantaneous power of the error signal $e_1(n)$, and P_{s_1} is the average power of the SI signal $s_1(i)$. We will also use the SI cancellation (SIC) factor given by

$$\mathrm{SIC} = \frac{P_{e_1}}{P_{\text{res}}}, \tag{6}$$

where P_{res} is the average power of the residual signal $r(n) = e_1(n) - v_1(n) - f(n)$. The baseband signals $v_1(n)$ and $f(n)$ are obtained as outputs of the complex demodulator in response to the passband signals $v_1(i)$ and $f(i)$, respectively. The signal-to-noise ratio (SNR) for the far-end signal is defined as

$$\mathrm{SNR}_{\text{far}} = \kappa \frac{P_f}{\sigma_{v_1}^2}, \tag{7}$$

where P_f is the average power of the received far-end signal $f(i)$ and $\sigma_{v_1}^2$ is the variance of the noise $v_1(i)$.

The signal $y(n) = e_1(n)$ after the acoustic SI cancellation is treated as an estimate of the far-end baseband signal $f(n)$.

III. SIMULATION RESULTS

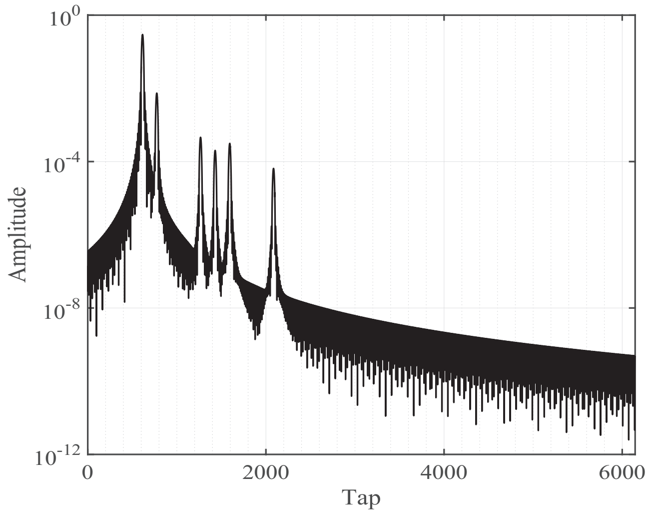

Fig. 5. Magnitude of the impulse response of the primary path ($\mathbf{h}_1$).

For the simulation, we use the version of the Waymark simulator presented in [19]. We consider a simulation scenario for transmission in a shallow sea of depth 50 m with a constant sound speed profile of 1500 m/s and flat sea surface. The hydrophone and transducers are positioned at a depth of 10 m. The primary transducer is 0.5 m away from the hydrophone, and the secondary transducer is 0.1 m away from the hydrophone. The impulse responses of the primary and secondary paths are shown in Fig. 5 and Fig. 6, respectively; the taps are measured in sampling intervals $T_s = 1/f_s$. Data sequences of $150 \cdot 1024$ QPSK symbols are transmitted and received simultaneously. The far-end channel is modelled as a single path channel.

The vectors $\hat{\mathbf{w}}_1$ and $\hat{\mathbf{w}}_2$ (adaptive filters 1 and 2) are of lengths $L_1 = 150$ and $L_2 = 55$, respectively.

Both the signals $s_1(i)$ and $s_2(i)$ are provided by the Waymark simulator. The noise signal $v_1(i)$ is added to the hydrophone to make the SI-to-noise ratio $\mathrm{SNR}_{\mathrm{SI}}$ between

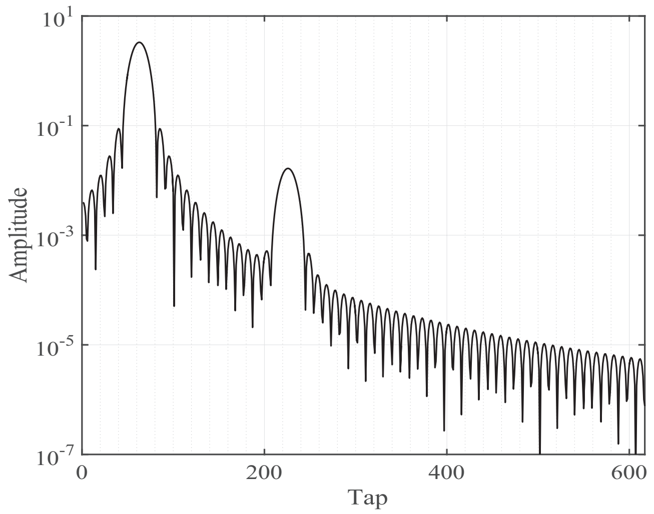

Fig. 6. Magnitude of the impulse response of the secondary path ($\mathbf{h}_2$).

the SI signal from the primary path and the noise equals to $\mathrm{SNR}_{\mathrm{SI}} = 100$ dB; it is defined as

$$\mathrm{SNR}_{\mathrm{SI}} = \kappa \frac{P_{s_1}}{\sigma^2_{v_1}}, \tag{8}$$

where P_{s_1} is the average power of the signal $s_1(i)$.

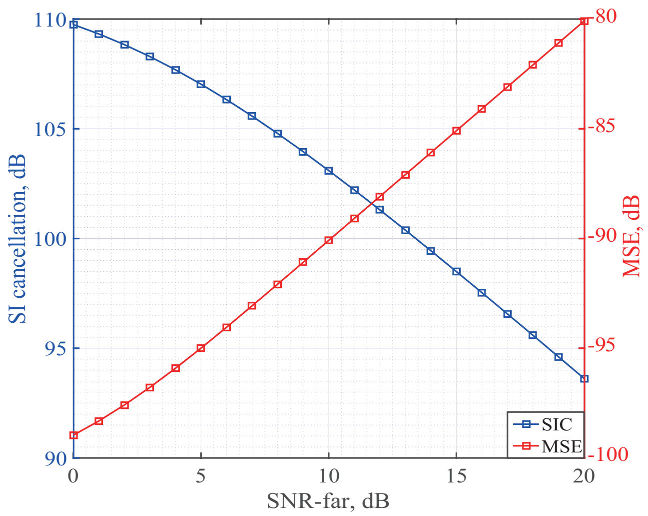

Fig. 7. MSE and SIC performance of the FD-UWAC system against the far-end SNR.

Fig. 7 shows the MSE and SIC performance. It can be seen that the MSE increases with $\mathrm{SNR}_{\mathrm{far}}$. This happens because the far-end signal introduces an extra interference to the SI canceller and the interference level increases with $\mathrm{SNR}_{\mathrm{far}}$. However, the proposed scheme provides the SIC factor higher than 100 dB at $\mathrm{SNR}_{\mathrm{far}} < 13$ dB. This indicates that the residual SI after the cancellation is below the noise level at $\mathrm{SNR}_{\mathrm{far}} < 13$ dB, and thus it should not much worsen the detection performance compared to the case without the SI.

Fig. 8 shows the BER performance of the proposed scheme for two cases. In Case 1, during adjustment of $\hat{\mathbf{w}}_1$, the far-end signal is present as discussed above. In Case 2, the adaptation is performed without the far-end signal, and thus the performance in this case should be improved. Indeed, we can observe this effect in Fig. 8. The presence of the far-end signal does degrade the detection performance; e.g., at $\mathrm{SNR}_{\mathrm{far}} = 15$ dB, the loss is about 3.5 dB. However, the QPSK transmission in our simulation does not use any coding. With the coding, the operating $\mathrm{SNR}_{\mathrm{far}}$ would reduce and the degradation in the detection performance would be lower.

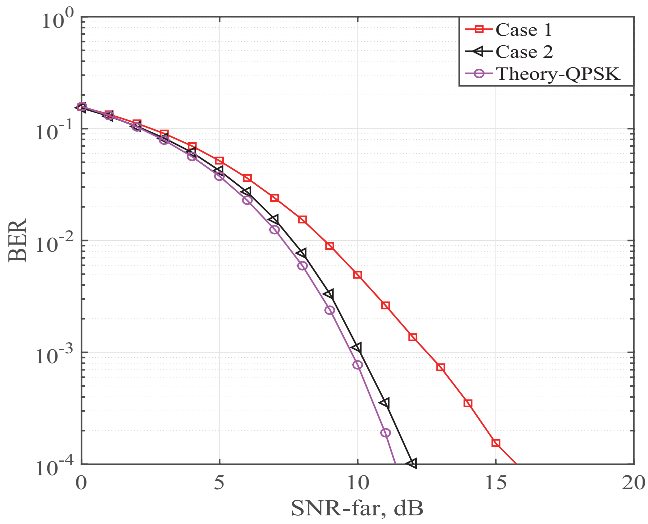

Fig. 8. BER performance of the FD-UWAC system with different levels of far-end SNR.

IV. Conclusions

In this paper, we propose a self-interference cancellation scheme for FD-UWAC systems. The SI cancellation is performed in the acoustic domain using an extra (secondary) transmit antenna that emits an acoustic signal for cancelling the SI at the receive antenna. Since the primary and secondary paths are unknown, they are adaptively estimated using RLS-DCD adaptive filters. Simulation results based on the Waymark virtual signal transmission show that the proposed scheme can achieve the cancellation performance high enough for a reliable communication using the single-carrier transmission with QPSK symbols.

Acknowledgment

This work was supported by the PhD Student Research and Innovation Fund of the Fundamental Research Funds for the Central Universities (HEUGIP201707) and National Key Research and Development Program of China (2016YFE0111100). The work of Y. Zakharov was supported in part by the U.K. EPSRC through Grants EP/P017975/1 and EP/R003297/1.

References

[1] M. Stojanovic and J. Preisig, “Underwater acoustic communication channels: Propagation models and statistical

characterization," *IEEE Communications Magazine*, vol. 47, no. 1, pp. 84–89, 2009.

[2] D. B. Kilfoyle and A. B. Baggeroer, "The state of the art in underwater acoustic telemetry," *IEEE Journal of Oceanic Engineering*, vol. 25, no. 1, pp. 4–27, 2002.

[3] D. Bharadia, E. Mcmilin, and S. Katti, "Full duplex radios," *Computer Communication Review*, vol. 43, no. 4, pp. 375–386, 2013.

[4] J. I. Choi, M. Jain, K. Srinivasan, P. Levis, and S. Katti, "Achieving single channel, full duplex wireless communication," in *Int. Conf. Mobile Computing and Networking (MOBICOM), Chicago, USA*, Sept 2010, pp. 1–12.

[5] M. B. El_Mashade and A. Aboshosha, "Active and passive self-interference cancellation techniques for full-duplex systems in the next generation (5G) of mobile communication networks," *Advances in Networks*, vol. 5, no. 51, pp. 14–21, 2017.

[6] V. Tapio and M. Sonkki, "Analog and digital self-interference cancellation for full-duplex transceivers," in *22th European Wireless Conference, Oulu, Finland*, 2016, pp. 247–251.

[7] J. R. Krier and I. F. Akyildiz, "Active self-interference cancellation of passband signals using gradient descent," in *24th IEEE Int. Symp. Personal, Indoor, and Mobile Radio Communications (PIMRC), London, UK*, 2013, pp. 1212–1216.

[8] M. A. Khojastepour and S. Rangarajan, "Wideband digital cancellation for full-duplex communications," in *Record of the 46th Asilomar Conference on Signals, Systems and Computers (ASILOMAR), Pacific Grove, USA*, 2012, pp. 1300–1304.

[9] S. Li and R. D. Murch, "An investigation into baseband techniques for single-channel full-duplex wireless communication systems," *IEEE Transactions on Wireless Communications*, vol. 13, no. 9, pp. 4794–4806, 2014.

[10] M. Duarte and A. Sabharwal, "Full-duplex wireless communications using off-the-shelf radios: Feasibility and first results," in *Record of the 44th Asilomar Conference on Signals, Systems and Computers, Pacific Grove, USA*, 2010, pp. 1558–1562.

[11] S. Achaleshwar, P. Gaurav, and S. Ashutosh, "Pushing the limits of full-duplex: Design and real-time implementation," *Rice University, Houston, TX, USA, Tech. Rep. TREE1104*, 2011.

[12] G. Qiao, S. Gan, S. Liu, L. Ma, and Z. Sun, "Digital self-interference cancellation for asynchronous in-band full-duplex underwater acoustic communication," *Sensors*, vol. 18, no. 6, pp. 1700, 2018.

[13] L. Li, A. Song, L. J. Cimini, and X. G. Xia, "Interference cancellation in in-band full-duplex underwater acoustic systems," in *MTS/IEEE OCEANS, Washington, USA*, 2015, pp. 1–6.

[14] G. Qiao, S. Liu, Z. Sun, and F. Zhou, "Full-duplex, multi-user and parameter reconfigurable underwater acoustic communication modem," in *MTS/IEEE OCEANS, San Diego, USA*, 2014, pp. 1–8.

[15] C. Liu, Y. V. Zakharov, and T. Chen, "Doubly selective underwater acoustic channel model for a moving transmitter/receiver," *IEEE Transactions on Vehicular Technology*, vol. 61, no. 3, pp. 938–950, 2012.

[16] G. L. Stüber, *Principles of mobile communication*, Springer Science & Business Media, 2011.

[17] Y. V Zakharov, G. P White, and J. Liu, "Low-complexity RLS algorithms using dichotomous coordinate descent iterations," *IEEE Transactions on Signal Processing*, vol. 56, no. 7, pp. 3150–3161, 2008.

[18] S. Haykin, *Adaptive Filter Theory, 3rd-ed*, Printice Hall, 1996.

[19] B. Henson, J. Li, Y. V. Zakharov, and C. Liu, "Waymark baseband underwater acoustic propagation model," in *2014 Underwater Communications and Networking (UComms), Sestri Levante, Italy, September*, 2014, pp. 1–5.